

**₁ How salty is the global ocean: weighing it all or
₂ tasting it a sip at a time?**

R. M. Ponte¹, Q. Sun¹, C. Liu², and X. Liang²

¹Atmospheric and Environmental
Research, Inc., Lexington, Massachusetts,
USA.

²School of Marine Science and Policy,
University of Delaware, Delaware, USA.

Key Point #1: Global mean salinity \bar{S} can be derived from space gravity and sea ice data, aside from conventional *in situ* salinity data

Key Point #2: Various \bar{S} series (2005–2019) show poor agreement for seasonal and longer variability, with unrealistic variations in *in situ* products

Key Point #3: Most *in situ* estimates have large biases since around 2015, which can explain recent discrepancies in global mean sea level budgets

Global ocean mean salinity \bar{S} is a key indicator of the Earth’s hydrological cycle and the exchanges of freshwater between land and ocean, but its determination remains a challenge. Aside from traditional methods based on gridded salinity fields derived from *in situ* measurements, we explore estimates of \bar{S} based on liquid freshwater changes derived from space gravimetry data corrected for sea ice effects. For the 2005–2019 period analyzed, the different \bar{S} series show little consistency in seasonal, interannual, and long-term variability. *In situ* estimates show sensitivity to choice of product and unrealistic variations. A suspiciously large rise in \bar{S} since ~ 2015 is enough to measurably affect halosteric sea level estimates and can explain recent discrepancies in the global mean sea level budget. Gravimetry-based \bar{S} estimates are more realistic, inherently consistent with estimated freshwater contributions to global mean sea level, and provide a way to calibrate the *in situ* estimates.

1. Introduction

The ability to accurately determine the temporal evolution of globally averaged ocean quantities (e.g., temperature, salinity, sea level) is essential for monitoring and predicting the Earth’s climate but ultimately difficult to achieve [Wunsch, 2016]. Despite strong advances made in the implementation of global, multi-platform (*in situ* and satellite) climate and ocean observing systems [Houghton *et al.*, 2012; Speich *et al.*, 2019], many challenges remain when trying to achieve sufficient coverage over the vast global oceans. Satellites can probe globally at reasonable sampling frequency but are very limited when it comes to measuring the ocean interior; *in situ* instruments can sample the subsurface but suffer from limited spatiotemporal coverage.

In any observational system, built-in redundancy, which allows the same quantity to be measured by two or more independent methods, is ideal for cross-calibration and uncertainty quantification. Such is the incipient case, for example, with global mean sea level: satellite altimetry on one hand and space gravity [Tapley *et al.*, 2019; Landerer *et al.*, 2020] and *in situ* Argo floats [Roemmich *et al.*, 2009, 2019] on the other provide two independent estimates that can be compared for consistency [Group, 2018]. These same observing platforms, which overlap since ~ 2002 despite some heterogeneity in spatiotemporal coverage, together with information on sea ice, can in principle be used to assess global mean ocean salinity \bar{S} [Munk, 2003] — a key indicator of the Earth’s freshwater budget, in particular the associated transfers between the ice and terrestrial water reservoirs and the ocean.

Llovel et al. [2019] have recently used *in situ* estimates of \overline{S} to check the trends in ocean mean mass inferred from the Gravity Recovery and Climate Experiment (GRACE) mission [Tapley et al., 2019], finding reasonable agreement between the two different measurements for the period 2005–2015. Assessing the variability at seasonal and interannual time scales is, however, also of primary interest in climate studies. In addition, given the evolution of all observational systems — e.g., new Argo floats [Roemmich et al., 2019], gaps and changes between GRACE and GRACE-Follow On missions [Landerer et al., 2020] — it is important to continuously monitor their consistency. Recent examination of sea level budgets portrayed by satellite altimeter, gravity, and *in situ* observations have pointed to substantial inconsistencies since ~ 2015 suggestive of problems with one or more of the data sets [Chen et al., 2020]. Here we assess if, over the most well-observed period since 2005, the *in situ* salinity and satellite gravity data can be the basis for accurate and consistent estimates of seasonal, interannual and long-term changes in \overline{S} or equivalently in global mean freshwater content in the oceans. Our findings have important implications for global mean sea level studies as well.

2. Data and Methods

2.1. Salinity Products

Five different gridded salinity fields [Liu et al., 2020], based on *in situ* data mostly from the Argo Program [Roemmich et al., 2009, 2019], were used to estimate \overline{S} . These Argo-based analyses are: the Barnes objective analysis (BOA) from the Chinese Second Institute of Oceanography [Li et al., 2017]; the EN4.2.1 product (or EN4 for short) from the UK Met Office [Good et al., 2013]; the variational interpo-

lation product from the International Pacific Research Center (IPRC) available from
<http://apdrc.soest.hawaii.edu/projects/argo/>; the Monthly Objective Analysis using
 Argo (MOAA) from the Japan Agency for Marine-Earth Science and Technology [*Hosoda et al.*, 2008]; and the Roemmich-Gilson (RG) Argo Climatology from the Scripps Institution of Oceanography [*Roemmich and Gilson*, 2009]. All datasets were available at and downloaded from <https://argo.ucsd.edu/data/argodata-products>. With the exception of MOAA and EN4, these analyses use exclusively Argo data to produce optimally interpolated fields at monthly intervals and a spatial resolution of 1° . The EN4 analysis provides near-global and full-depth coverage, while the others are essentially restricted to latitudes 60°N – 60°S and to depths shallower than 2000 m. For all these products, \bar{S} is estimated as the volume-weighted average of the available salinity fields for the period 2005–2019. For EN4, aside from full depth estimates, values of \bar{S} based on the upper 2000 m are also provided (denoted as EN4-2k).

2.2. Gravity Data

Global mean monthly series, representing the combined total mass of ocean plus sea ice and overlying snow, are derived from both GRACE and GRACE-Follow On missions [*Wiese et al.*, 2019]. The data, accessed on February 24, 2020, are based on the Jet Propulsion Laboratory mascon solutions [*Watkins et al.*, 2015] that use the Coastal Resolution Improvement filter. Available monthly values from 2002 to 2019 are used in this work, with no attempt to fill missing values due to data dropout and the gap between GRACE and GRACE-Follow On missions [*Wiese et al.*, 2019]. The error standard deviations provided with the time series are typically < 0.5 mm.

2.3. Sea Ice and Snow Products

For continuous, global values of sea ice and snow volume over the period of analysis, we use two different estimates both based on ocean-sea ice models constrained by data assimilation. In one case, monthly gridded effective sea ice thickness and water equivalent snow depth data are produced by the Global Ice/Ocean Modeling and Assimilation System (GIOMAS) and based on the global Parallel Ocean and sea Ice Model (POIM), run with data assimilation [Zhang and Rothrock, 2003]. Values for the period 2005–2019 were downloaded from https://pscfiles.apl.uw.edu/zhang/Global_seaice/. The equivalent water thickness from the combined sea ice and snow is calculated by multiplying the respective values by the GIOMAS grid-cell areas, summing over the domain and dividing by the global ocean surface area ($3.6 \times 10^{14} \text{ m}^2$).

A similar calculation is performed using the sea ice and snow thickness fields from the state estimates produced by the Estimating the Circulation and Climate of the Ocean (ECCO) project. The ECCO Version 4 Release 4 [ECCO et al., 2020; Forget et al., 2015] used here covers the period 1992–2017 and assimilates a variety of observations including in situ temperature and salinity profiles, satellite sea surface temperature, salinity and height, and ocean bottom pressure from GRACE and GRACE-Follow On. Output was downloaded from <https://ecco.jpl.nasa.gov/drive/files/Version4/Release4>.

3. Monitoring Changes in \bar{S}

Estimating \bar{S} from *in situ* measurements involves mapping the sparse sampling into a globally gridded field and integrating over the volume covered by the data. Quasi-global sampling was only achieved after the Argo Program reached maturity ~ 2005 [Roemmich

et al., 2009]. Nevertheless, one major issue is still the poor coverage below 2000 m and also at high latitudes, particularly those covered by sea ice, and shallow coastal regions, including marginal seas. Another issue is the aliasing of undersampled small scales onto the spatial mean.

The five gridded salinity products from different groups described in section 2.1, based primarily on Argo profiles but also using other data, and commonly analyzed in salinity studies [Llovel *et al.*, 2019; Liu *et al.*, 2020], are used here to estimate \bar{S} for the period 2005–2019. A comparison of all the monthly series (Fig. 1) reveals a wide spread in variability, which indicates considerable sensitivity of \bar{S} estimates to the choice of data and their quality control as well as mapping methods. Differences in the EN4 curves for full depth and 2000 m integrals also suggest sensitivity to vertical coverage. The IPRC series shows a couple of extreme low values, while all series except RG exhibit substantial increases after ~ 2015 . Apart from these features, there is no clear seasonal cycle in a relatively large month-to-month variability that seems somewhat incoherent among the different series.

An alternative method for calculating \bar{S} essentially amounts to monitoring changes in the weight of the ocean, which represent the net exchange of freshwater with the land, atmosphere and cryosphere (assuming negligible changes in salt content). Expressing changes in freshwater as an equivalent water thickness change δh^{fw} , the fractional change in \bar{S} is approximately equal and of opposite sign to the fractional change in ocean volume or mean depth [Munk, 2003; Wunsch, 2018], i.e.,

$$\delta \bar{S} \simeq -\bar{S}_0 \frac{\delta h^{fw}}{H_0} \quad (1)$$

with \bar{S}_0 being a reference mean salinity value and H_0 being the average ocean depth. The launch of GRACE in 2002 and the Follow-On mission in 2018 [Tapley et al., 2019; Landerer et al., 2020] essentially provides a measure of $\delta h^{fw} + \delta h^{si}$, where δh^{si} represents changes in freshwater contained in floating sea ice and snow, in equivalent water thickness. Inferring δh^{fw} from gravity data requires a separate estimate of δh^{si} . In addition, although gravity measurements are truly global, coarse spatial resolution (~ 300 km) can make it difficult to separate land and ocean mass changes [Watkins et al., 2015].

The monthly time series of $\delta h^{fw} + \delta h^{si}$ in Fig. 2, based on GRACE and GRACE-Follow On data described in section 2.2, shows a clear upward trend of ~ 2 mm/yr and a seasonal cycle of ~ 1 cm amplitude and maximum in September/October, with weaker interannual fluctuations. The observed variability, corresponding to that of barystatic sea level, is within the expected bounds provided by independent satellite measurements of global mean sea level, which contain also the effects of changes in global mean thermosteric changes [Group, 2018].

Separate estimates of δh^{si} , obtained from the ECCO and GIOMAS ocean/sea ice data assimilation products described in section 2.3, can be used to remove effects of changes in sea ice and snow mass from the space gravity measurements. The resulting δh^{fw} series (Fig. 2) shows a considerably larger seasonal cycle, representing a strong seasonality in δh^{si} that is out-of-phase with δh^{fw} (i.e., changes in sea ice and snow mass result in opposite changes in ocean freshwater content, as expected from a primary exchange between the two reservoirs). In contrast, only a slightly more positive trend results from removing effects of δh^{si} , representing a relatively small decrease in sea ice and snow mass over the

period of analysis. Differences in the ECCO- and GIOMAS-based δh^{fw} series are most evident at the seasonal timescale: GIOMAS has a stronger seasonal cycle in sea ice over the Southern Ocean, which leads to a larger annual peak in δh^{fw} . Such differences give a sense of uncertainty in available δh^{si} estimates.

4. Assessing \bar{S} Series

How consistent are the *in situ* estimates of \bar{S} in Fig. 1 and those that can be inferred from δh^{fw} values in Fig. 2? We examine separately the mean seasonal cycle, interannual variability, and long term trends. Values of δh^{fw} are converted to changes in \bar{S} using (1) with $H_0 = 3682$ m [Charette and Smith, 2010] and $\bar{S}_0 = 34.7$ g/kg [Wunsch, 2018].

The mean seasonal cycle, calculated by averaging all the January, February,...,December values for each series (Fig. 3), exhibits widely different behavior among the *in situ* products. Curves from EN4, IPRC and BOA contain a visible annual cycle, but times of high and low \bar{S} can differ by up to 3 months. No apparent annual cycle is seen for MOAA series. The seasonal cycle for RG is weaker with a minimum in March but no clear maximum. Compared to *in situ* series, the seasonal cycle based on estimates of δh^{fw} tends to be weaker and smoother, with high \bar{S} in May and low \bar{S} in September; accounting for sea ice effects introduces noticeable phase deviations from a pure annual cycle (Fig. 3). There is little agreement with most *in situ* series. The closest match is with EN4, although the latter has substantially larger amplitudes and is shifted in phase by at least one month. Using ECCO or GIOMAS for the δh^{si} correction yields relatively minor differences, compared to the spread in *in situ* \bar{S} .

Interannual variability (Fig. 4) shows a large range ($\sim 5 \times 10^{-3}$) for *in situ* estimates, which is equivalent to freshwater thickness changes of ~ 50 cm! As noticed in Fig. 1, a large part of this range is due to the rise in \bar{S} after 2015, which is clear for all *in situ* series except RG. Such rise is likely related to known but not easily removable salinity biases in some batches of recently deployed Argo floats [Roemmich *et al.*, 2019]. The RG product seems to have stricter quality control of the affected instruments. In any case, typical year-to-year changes of several cm are seen in all *in situ* series. Over all, the interannual variations in *in situ* \bar{S} estimates are clearly unrealistic when compared to observed variability in global mean sea level [Group, 2018]. The interannual variability for δh^{fw} -based series is more than an order of magnitude smaller. The most conspicuous change is the long term negative trend in \bar{S} , with the effects of sea ice adding visible year-to-year variations, particularly in the second half of the record.

Linear trends in *in situ* \bar{S} calculated for 2005–2019 (Table 1) are largely affected by the apparent systematic biases after ~ 2015 . Trends for 2005–2015 are much smaller, except for IPRC and MOAA series, which show still unrealistic positive values. Negative trends are seen for EN4 and RG series, but with considerable uncertainty. The GRACE-derived estimates, in contrast, indicate a decrease in \bar{S} stable across both periods and clearly distinguishable from zero, given formal trend errors. Effects of sea ice are relatively small for 2005–2015, but tend to yield a stronger negative trend over 2005–2019, suggesting an increased role of sea ice melting in \bar{S} changes in most recent years.

5. Interpretation and Conclusions

The spread in behavior among all *in situ* \bar{S} estimates, for all time scales examined (Figs. 3 and 4, Table 1), indicates their sensitive dependence on particular choice of data, quality control procedures, and mapping methods. These sensitivities are exacerbated by the acknowledged sparse *in situ* data sampling, including deep and high latitude regions with very little measurements. As already noted, including depths > 2000 m makes a visible difference in the case of the two EN4 series, both for the seasonal cycle (Fig. 3) and the interannual variability (Fig. 4). Given that not much seasonal variability is expected in the abyssal ocean, such differences are suggestive of sampling issues.

Horizontal data coverage can be equally important. Restricting the volume integral of EN4 salinities to lower latitudes, corresponding to the horizontal extent of Argo-based products, leads to substantial changes particularly for the seasonal cycle (not shown), indicating that changes in salinity at high latitudes are important to determine \bar{S} . The finding is consistent with the result that seasonal variations in sea ice mass contribute substantially to the total freshwater content in the oceans (Fig. 2).

Most importantly, results also indicate that *in situ* values of \bar{S} can have systematic biases. These biases are large enough to affect estimates of global mean steric sea level. In particular, the spurious rise in \bar{S} after 2015, seen in all series except RG, is equivalent to δh^{fw} changes of ~ 20 – 40 cm (Fig. 4). Using Munk’s factor of $1/36.7$ to convert δh^{fw} to halosteric sea level [Munk, 2003] yields a decrease of the order of 5 – 10 mm. This is of the same magnitude and sign of discrepancies seen in comparisons between global mean sea level altimeter estimates corrected for steric effects and barystatic sea level

based on GRACE and GRACE-FO data [Chen *et al.*, 2020]. Our analyses indicate that a considerable portion of discrepancies found in Chen *et al.* [2020] can be explained by the biased *in situ* salinity data since 2015.

Estimates based on δh^{fw} measurements, which are consistent with contributions of freshwater to global mean sea level budgets [Group, 2018], provide at this point a more reliable method to arrive at \bar{S} than the *in situ* measurements. In particular, long term trends and interannual signals are relatively weak and can be overwhelmed by issues with *in situ* sampling. The δh^{fw} -based estimates of \bar{S} can serve as a consistency check on *in situ* measurements, revealing potential unknown biases and providing a way to cross-calibrate those data. Cross-calibration of gravity-based estimates of $\delta h^{fw} + \delta h^{si}$ is already routinely carried out against independent estimates obtained from differencing global mean sea level and thermosteric sea level, calculated from satellite altimetry and Argo temperatures, respectively [Group, 2018].

We have explored how having estimates of $\delta h^{fw} + \delta h^{si}$ from space-based methods and separate knowledge of δh^{si} can allow one to estimate \bar{S} . Knowledge about δh^{si} is, however, also scarce. Conversely, having a good estimate of \bar{S} from *in situ* measurements, one could use its equivalent δh^{fw} values to remove effects of ocean freshwater content on the space gravity estimates to arrive at improved values of δh^{si} . Improvements in sampling from *in situ* measurements, including the implementation of deep profiling floats and better coverage of high latitude, ice-prone regions, promise to provide further redundancy and consistency checks on all these essential climate variables.

Acknowledgments. Work was supported by the NASA GRACE Follow-On Science Team (grant 80NSSC20K0728) and the US NSF (grant OCE-2021274). The ECCO project is funded by the NASA Physical Oceanography, Cryospheric Science, and Modeling, Analysis and Prediction programs. All data used in this study are publicly available at the following sites: salinity (<https://argo.ucsd.edu/data/argodata-products/>); GIOMAS sea ice (https://pscfiles.apl.uw.edu/zhang/Global_seaice/); ECCO sea ice (<https://ecco.jpl.nasa.gov/drive/files/Version4/Release4/>); GRACE and GRACE-FO (https://podaac.jpl.nasa.gov/dataset/TELLUS_GRAC-GRFO_MASCON_CRI_GRID_RL06_V2).

References

- Charette, M. A., and W. H. Smith (2010), The volume of Earth’s ocean, *Oceanography*, *23*(2).
- Chen, J., B. Tapley, C. Wilson, A. Cazenave, K.-W. Seo, and J.-S. Kim (2020), Global ocean mass change from GRACE and GRACE Follow-On and altimeter and Argo measurements, *Geophysical Research Letters*, *47*(22), e2020GL090,656, doi: <https://doi.org/10.1029/2020GL090656>.
- ECCO, C., I. Fukumori, O. Wang, I. Fenty, G. Forget, P. Heimbach, and R. M. Ponte (2020), Synopsis of the ECCO central production global ocean and sea-ice state estimate, doi:10.5281/zenodo.3765929.
- Forget, G., J.-M. Campin, P. Heimbach, C. N. Hill, R. M. Ponte, and C. Wunsch (2015), ECCO version 4: an integrated framework for non-linear inverse modeling and global ocean state estimation, *Geoscientific Model Development*, *8*(10), 3071–3104, doi: 10.5194/gmd-8-3071-2015.

- Good, S. A., M. J. Martin, and N. A. Rayner (2013), EN4: Quality controlled ocean temperature and salinity profiles and monthly objective analyses with uncertainty estimates, *Journal of Geophysical Research: Oceans*, *118*(12), 6704–6716, doi: <https://doi.org/10.1002/2013JC009067>.
- Group, W. G. S. L. B. (2018), Global sea-level budget 1993–present, *Earth System Science Data*, *10*(3), 1551–1590, doi:10.5194/essd-10-1551-2018.
- Hosoda, S., T. Ohira, and T. Nakamura (2008), A monthly mean dataset of global oceanic temperature and salinity derived from Argo float observations, *JAMSTEC Report of Research and Development*, *8*, 47–59, doi:10.5918/jamstecr.8.47.
- Houghton, J., J. Townshend, K. Dawson, P. Mason, J. Zillman, and A. Simmons (2012), The GCOS at 20 years: the origin, achievement and future development of the Global Climate Observing System, *Weather*, *67*(9), 227–235, doi: <https://doi.org/10.1002/wea.1964>.
- Landerer, F. W., F. M. Flechtner, H. Save, F. H. Webb, T. Bandikova, W. I. Bertiger, S. V. Bettadpur, S. H. Byun, C. Dahle, H. Dobslaw, E. Fahnestock, N. Harvey, Z. Kang, G. L. H. Kruizinga, B. D. Loomis, C. McCullough, M. Murböck, P. Nagel, M. Paik, N. Pie, S. Poole, D. Strelakov, M. E. Tamisiea, F. Wang, M. M. Watkins, H.-Y. Wen, D. N. Wiese, and D.-N. Yuan (2020), Extending the global mass change data record: GRACE Follow-On instrument and science data performance, *Geophysical Research Letters*, *47*(12), e2020GL088,306, doi:<https://doi.org/10.1029/2020GL088306>.
- Li, H., F. Xu, W. Zhou, D. Wang, J. S. Wright, Z. Liu, and Y. Lin (2017), Development of a global gridded Argo data set with Barnes successive corrections, *Journal of Geophysical*

- 273 *Research: Oceans*, 122(2), 866–889, doi:<https://doi.org/10.1002/2016JC012285>.
- 274 Liu, C., X. Liang, D. P. Chambers, and R. M. Ponte (2020), Global patterns of spatial
275 and temporal variability in salinity from multiple gridded Argo products, *Journal of*
276 *Climate*, 33(20), 8751 – 8766, doi:10.1175/JCLI-D-20-0053.1.
- 277 Llovel, W., S. Purkey, B. Meyssignac, A. Blazquez, N. Kolodziejczyk, and J. Bamber
278 (2019), Global ocean freshening, ocean mass increase and global mean sea level rise
279 over 2005–2015, *Scientific Reports*, 9(1), doi:10.1038/s41598-019-54239-2.
- 280 Munk, W. (2003), Ocean freshening, sea level rising, *Science*, 300(5628), 2041–2043, doi:
281 10.1126/science.1085534.
- 282 Roemmich, D., and J. Gilson (2009), The 2004–2008 mean and annual cycle of tempera-
283 ture, salinity, and steric height in the global ocean from the Argo Program, *Progress in*
284 *Oceanography*, 82(2), 81–100, doi:<https://doi.org/10.1016/j.pocean.2009.03.004>.
- 285 Roemmich, D., G. C. Johnson, S. Riser, R. Davis, J. Gilson, W. B. Owens, S. L. Garzoli,
286 C. Schmid, and M. Ignaszewski (2009), The Argo Program: Observing the global ocean
287 with profiling floats, *Oceanography*, 22(2), 34–43.
- 288 Roemmich, D., M. H. Alford, H. Claustre, K. Johnson, B. King, J. Moum, P. Oke,
289 W. B. Owens, S. Pouliquen, S. Purkey, M. Scanderbeg, T. Suga, S. Wijffels, N. Zilber-
290 man, D. Bakker, M. Baringer, M. Belbeoch, H. C. Bittig, E. Boss, P. Calil, F. Carse,
291 T. Carval, F. Chai, D. O. Conchubhair, F. d’Ortenzio, G. Dall’Olmo, D. Desbruyeres,
292 K. Fennel, I. Fer, R. Ferrari, G. Forget, H. Freeland, T. Fujiki, M. Gehlen, B. Greenan,
293 R. Hallberg, T. Hibiya, S. Hosoda, S. Jayne, M. Jochum, G. C. Johnson, K. Kang,
294 N. Kolodziejczyk, A. Körtzinger, P.-Y. L. Traon, Y.-D. Lenn, G. Maze, K. A. Mork,

295 T. Morris, T. Nagai, J. Nash, A. N. Garabato, A. Olsen, R. R. Pattabhi, S. Prakash,
296 S. Riser, C. Schmechtig, C. Schmid, E. Shroyer, A. Sterl, P. Sutton, L. Talley, T. Tan-
297 hua, V. Thierry, S. Thomalla, J. Toole, A. Troisi, T. W. Trull, J. Turton, P. J. Velez-
298 Belchi, W. Walczowski, H. Wang, R. Wanninkhof, A. F. Waterhouse, S. Waterman,
299 A. Watson, C. Wilson, A. P. S. Wong, J. Xu, and I. Yasuda (2019), On the future
300 of Argo: A global, full-depth, multi-disciplinary array, *Frontiers in Marine Science*, 6,
301 439, doi:10.3389/fmars.2019.00439.

302 Speich, S., T. Lee, F. Muller-Karger, L. Lorenzoni, A. Pascual, D. Jin, E. Delory,
303 G. Reverdin, J. Siddorn, M. R. Lewis, N. Marba, P. L. Buttigieg, S. Chiba, J. Manley,
304 A. T. Kabo-Bah, K. Desai, and A. Ackerman (2019), Editorial: Oceanobs'19: An ocean
305 of opportunity, *Frontiers in Marine Science*, 6, 570, doi:10.3389/fmars.2019.00570.

306 Tapley, B. D., M. M. Watkins, F. Flechtner, C. Reigber, S. Bettadpur, M. Rodell, I. Sas-
307 gen, J. S. Famiglietti, F. W. Landerer, D. P. Chambers, J. T. Reager, A. S. Gardner,
308 H. Save, E. R. Ivins, S. C. Swenson, C. Boening, C. Dahle, D. N. Wiese, H. Dobs law,
309 M. E. Tamisiea, and I. Velicogna (2019), Contributions of GRACE to understanding
310 climate change, *Nature Climate Change*, 9(5), 358–369, doi:10.1038/s41558-019-0456-2.

311 Watkins, M. M., D. N. Wiese, D.-N. Yuan, C. Boening, and F. W. Landerer (2015),
312 Improved methods for observing Earth's time variable mass distribution with GRACE
313 using spherical cap mascons, *Journal of Geophysical Research: Solid Earth*, 120(4),
314 2648–2671, doi:https://doi.org/10.1002/2014JB011547.

315 Wiese, D. N., D.-N. Yuan, C. Boening, F. W. Landerer, and M. M. Watkins (2019),
316 JPL GRACE and GRACE-FO Mascon Ocean, Ice, and Hydrology Equivalent Water

Height Coastal Resolution Improvement (CRI) Filtered Release 06 Version 02, doi:
10.5067/TEMSC-3JC62.

Wunsch, C. (2016), Global ocean integrals and means, with trend implications, *Annual Review of Marine Science*, 8(1), 1–33, doi:10.1146/annurev-marine-122414-034040.

Wunsch, C. (2018), Towards determining uncertainties in global oceanic mean values of heat, salt, and surface elevation, *Tellus A: Dynamic Meteorology and Oceanography*, 70(1), 1–14, doi:10.1080/16000870.2018.1471911.

Zhang, J., and D. A. Rothrock (2003), Modeling global sea ice with a thickness and enthalpy distribution model in generalized curvilinear coordinates, *Monthly Weather Review*, 131(5), 845–861, doi:10.1175/1520-0493(2003)131;0845:MGSIIWA;2.0.CO;2.

Table 1. Linear Trends and Standard Errors for \bar{S} (10^{-4} g/kg/year).^a

Products	2005–2019	2005–2015
BOA	2.37 ± 0.20	0.12 ± 0.17
EN4	1.41 ± 0.13	-0.14 ± 0.16
EN4-2k	2.95 ± 0.24	0.04 ± 0.27
IPRC	3.06 ± 0.18	1.82 ± 0.23
MOAA	3.25 ± 0.15	1.66 ± 0.17
RG	0.35 ± 0.12	-0.12 ± 0.18
GRACE	-0.21 ± 0.01	-0.22 ± 0.02
GRACE– δh^{si} (ECCO)	-0.22 ± 0.03	-0.21 ± 0.04
GRACE– δh^{si} (GIOMAS)	-0.25 ± 0.02	-0.20 ± 0.03

^a Values given for various *in situ* and gravity-based estimates of \bar{S} . Calculations are based on annual mean series in Fig. 4. Value in bold represents the period 2005–2017.

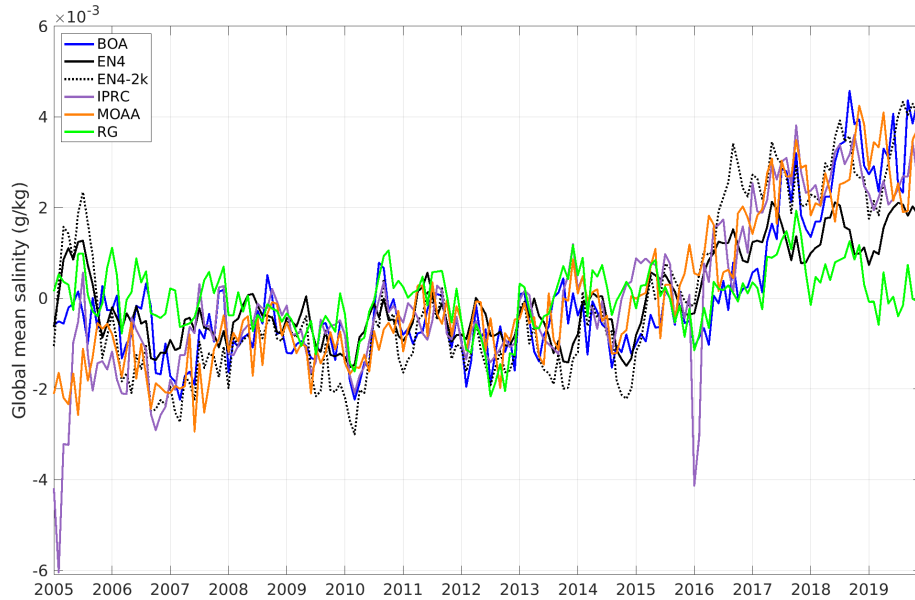


Figure 1. Monthly time series of \bar{S} calculated from five different gridded *in situ* salinity products: BOA [Li et al., 2017], EN4 [Good et al., 2013], IPRC (<http://apdrc.soest.hawaii.edu/projects/argo/>), MOAA [Hosoda et al., 2008], and RG [Roemmich and Gilson, 2009]. The EN4 series is the only based on a global product; EN4-2k uses only values over the upper 2000 m, similar to the other series.

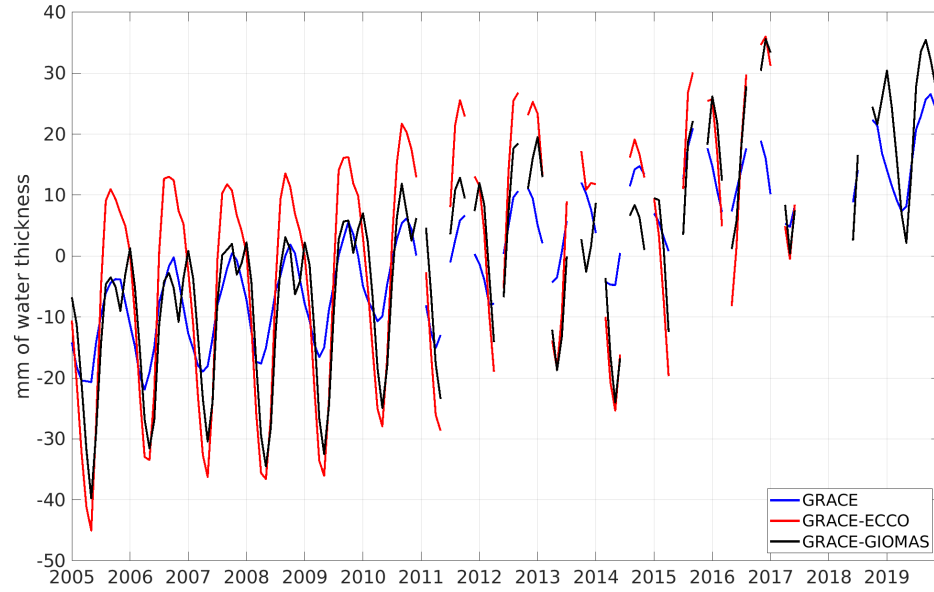


Figure 2. Monthly time series of $\delta h^{fw} + \delta h^{si}$, in mm of water thickness, based on GRACE and GRACE-FO measurements, and δh^{fw} , based on latter series corrected by estimates of sea ice and snow thickness δh^{si} from the ECCO and GIOMAS data assimilation products. Gaps in the gravity data are left blank.

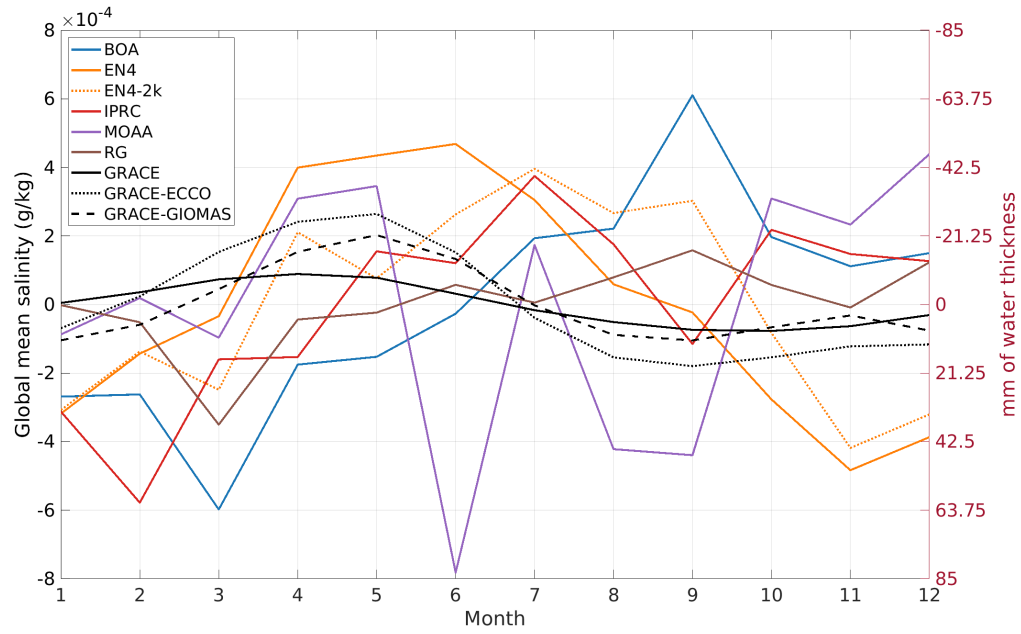


Figure 3. Mean seasonal cycle in \bar{S} (g/kg) for all *in situ* and GRACE-based estimates shown in Figs. 1 and 2. Month 1 corresponds to January. Equivalent changes in freshwater content, in mm of water thickness, are given on the right y-axis.

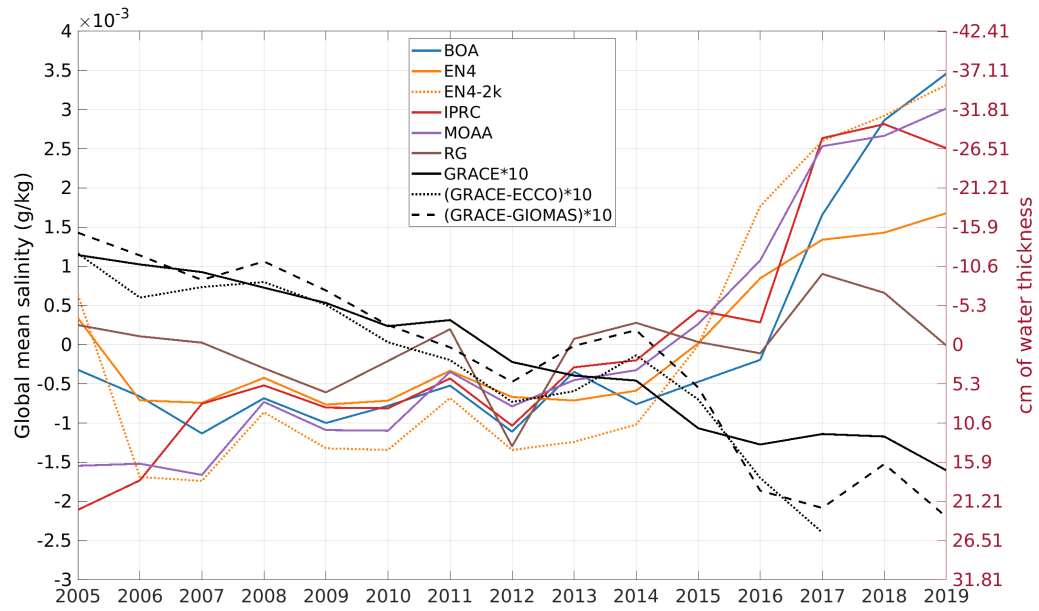


Figure 4. Annual mean \bar{S} series for various products as in Fig. 3. The curves based on gravity data have been multiplied by 10 for better visualization.